DOI:10.3969/j.issn.1005-202X.2018.05.014

医学影像物理

磁共振动态增强扫描、ADC及3D减影技术对卵巢囊腺瘤和囊腺癌的诊断价值

吴梦楠[1,2]，全显跃[1]，黄志明[2]，柯灿泽[2]，赖东平[2]
1.南方医科大学珠江医院放射科，广东 广州 510280；2.河源市人民医院放射科，广东 河源 517000

【摘 要】目的：探讨磁共振动态增强扫描、多b值扩散加权成像(DWI)结合表现扩散系数(ADC)值及3D减影技术对卵巢囊腺瘤和囊腺癌的诊断价值。**方法：**对经手术病理证实的39例囊腺瘤和12例囊腺癌进行常规MRI、多b值DWI及肿瘤囊实性成分ADC测量、动态增强、3D减影多模态扫描资料进行回顾性分析。**结果：**55个病灶中，40个为良性囊腺瘤，15个为囊腺癌。常规MRI，51例中9例见彩色玻璃征，6例囊腺瘤在T_2WI见等信号壁结节。DWI在b值100、500、1 000 mm^2/s，卵巢囊腺癌的囊、实性部分ADC低于囊腺瘤瘤体，囊腺瘤ADC分别为(3.03±0.23)×10^{-3}、(2.92±0.20)×10^{-3}、(2.88±0.21)×10^{-3} mm^2/s，囊腺癌囊性ADC分别为(2.71±0.31)×10^{-3}、(2.63±0.27)×10^{-3}、(2.47±0.41)×10^{-3} mm^2/s，囊腺癌实性ADC分别为(1.80±0.50)×10^{-3}、(1.47±0.48)×10^{-3}、(1.30±0.39)×10^{-3} mm^2/s，囊腺瘤的瘤体与囊腺癌的囊、实性ADC值差异均有统计学意义(P<0.05)。动态增强扫描示囊腺瘤在T_2WI等信号壁结节无强化或轻度强化，TIC曲线呈I型，13个囊腺癌在T_2WI等信号壁结节、实性成分呈明显强化，TIC曲线呈II型，2个交界性囊腺癌TIC曲线呈I型。3D减影清楚显示壁结节动脉期强化特点，囊腺瘤乳头结构轻度强化，血栓及细胞碎片无强化，囊腺癌壁结节及肿块明显强化。**结论：**磁共振动态增强扫描、多b值DWI所表现ADC值、3D减影技术三者联合运用对评估卵巢囊腺瘤和囊腺癌价值更大。

【关键词】囊腺瘤；囊腺癌；磁共振扩散成像；表观扩散系数；动态增强扫描；3D减影技术
【中图分类号】R816.91 **【文献标志码】**A **【文章编号】**1005-202X(2018)05-0573-07

Value of dynamic contrast-enhanced MRI, ADC and 3D subtraction technique for the diagnosis of ovarian cystadenoma and cystadenocarcinoma

WU Mengnan[1,2], QUAU Xianyue[1], HUANG Zhiming[2], KE Canze[2], LAI Dongping[2]
1. Department of Radiology, Zhujiang Hospital, Southern Medical University, Guangzhou 510280, China; 2. Department of Radiology, Heyuan People's Hospital, Heyuan 517000, China

Abstract: Objective To explore the diagnostic value of dynamic contrast-enhanced magnetic resonance imaging (MRI), multiple b-value diffusion-weighted imaging (DWI) combined with apparent diffusion coefficient (ADC) and three-dimensional (3D) subtraction technique for ovarian cystadenoma and cystadenocarcinoma. **Methods** Thirty-nine cases of cystadenoma and 12 cases of cystadenocarcinoma confirmed by surgery and pathology received conventional MRI, multiple b-value DWI with ADC measurement of solid and cystic components, dynamic contrast-enhanced MRI, 3D subtraction multimodal scanning. The obtained data were retrospectively analyzed. **Results** Among 55 lesions, 40 of them were benign cystadenoma and the other 15 were cystadenocarcinoma. The conventional MRI revealed that among 51 selected cases, 9 cases had "stained-glass" sign and 6 cases of cystadenoma had isointensity wall nodules on T_2-weighted image (T_2WI). The b-value DWI was 100, 500, 1 000 mm^2/s, respectively. The ADC values of solid and cystic components of ovarian cystadenocarcinoma were lower than those of ovarian cystadenoma, with significant differences (P<0.05). The ADC values of cystadenoma were (3.03±0.23)×10^{-3}, (2.92±0.20)×10^{-3} and (2.88±0.21)×10^{-3} mm^2/s, respectively, while those of cystic components of cystadenocarcinoma were (2.71±0.31)×10^{-3}, (2.63±0.27)×10^{-3} and (2.47±0.41)×10^{-3} mm^2/s, respectively. The ADC values of solid components of cystadenocarcinoma were (1.80±0.50)×10^{-3}, (1.47±0.48)×10^{-3} and (1.30±0.39)×10^{-3} mm^2/s, respectively. The dynamic contrast-enhanced MRI demonstrated that no enhancement or slightly enhancement on isointensity wall nodules on T_2WI of cystadenoma, and the time-intensity curve

【收稿日期】2018-02-10
【基金项目】河源市科技局社会发展科技计划项目(河科[2016]56号)
【作者简介】吴梦楠，硕士，E-mail: 4863286@qq.com
【通信作者】全显跃，主任医师，E-mail: quanxianyue@163.com

(TIC) was type I. Moreover, the isointensity wall nodules and solid components in 13 cases of cystadenocarcinoma were significantly enhanced on T_2WI, and the TIC was type II. The TIC of 2 borderline cystadenocarcinoma was type I. 3D subtraction scanning image showed enhancement characteristics at the arterial phase of wall nodules. No enhancement was found at thrombus and cell fragments. The nipple structure of cystadenoma was slightly enhanced but the wall nodules and solid component of cystadenocarcinoma were significantly enhanced. **Conclusion** The combined use of dynamic contrast-enhanced MRI, multiple b-value DWI and 3D subtraction technique is more valuable for the diagnosis of ovarian cystadenoma and cystadenocarcinoma.
Keywords: cystadenoma; cystadenocarcinoma; diffusion-weighted imaging; apparent diffusion coefficient; dynamic contrast-enhanced magnetic resonance imaging; three-dimensional subtraction technique

前 言

卵巢表面上皮性间质肿瘤根据上皮不同细分为5大类：浆液性、黏液性、子宫内膜样、透明细胞性、移行细胞型，约占全部卵巢肿瘤的70%~75%，其发病率逐年上升且不断年轻化，恶性者预后不良，因此对其早期诊断及评估具有重要意义。目前扩散加权成像(DWI)在临床肿瘤良恶性的鉴别诊断中广泛运用，具有一定优势[1]，但对于肿瘤实性肿块的DWI弥散受限呈高信号预示恶性肿瘤的准确性并不高[2]。动态增强扫描及时间-强化曲线(TIC)类型广泛用于鉴别乳腺良恶性肿瘤[3-4]。肿瘤壁结节及实性肿块强化所形成的TIC类型及3D减影增强T_1WI显示强化特点，可以弥补DWI及表现扩散系数(ADC)值不足，增加鉴别良恶性肿瘤的把握性，提高准确率。本研究着重探讨磁共振动态增强扫描(DCE)及TIC类型结合多b值DWI结合ADC值、3D减影技术鉴别卵巢囊腺瘤和囊腺癌的价值。

1 资料与方法

1.1 临床资料

收集2016年1月~2018年1月经手术病理证实的卵巢囊腺瘤和囊腺癌患者51例，年龄19~79岁，平均(47.3±16.4)岁，临床主要症状为腹胀、腹痛、盆腔或腹部肿块，以腹胀、腹部包块来诊24例，腹痛14例，月经改变2例，体检发现11例。39例囊腺瘤中5例CA125轻度增高，1例CA199、1例CEA轻度增高；12例囊腺癌CA125均明显增高(>3倍正常值)。

1.2 仪器与方法

采用GE Signa HDxt1.5T扫描仪，行盆腔常规MRI扫描、DWI及动态增强扫描，扫描范围从髂嵴至耻骨联合，常规横断面、冠状面、矢状面行TSE快速自旋回波，T_1WI(TR/TE：520 ms/9 ms)，T_2WI(TR/TE：2 320 ms/110 ms)及压脂T_2WI(TR/TE：2 700 ms/71 ms)，DWI采用自旋回波平面回波(EPI)，b值取100、500、1 000 mm^2/s(TR/TE：4000~5100 ms/49~77 ms)，层厚/层间距：5~6 mm/6~7 mm，动态增强层厚/层间距：4 mm/2 mm，FOV：24 cm×24 cm~36 cm ×36 cm，矩阵：288×224，增强扫描采用Gd-DTPA，注射流速1.5~2.0 mL/s，剂量0.1 mmol/kg。

1.3 设置ADC值的感兴趣区(ROI)

b=100、500、1 000 mm^2/s，DWI扫描后由2名主治医师后处理ADC图像，在囊腺瘤囊体区与囊腺癌囊、实性部分最大层面上手动选取ROI，ROI需与组织边缘相隔5 mm，每个b值所得ADC图测量3次，分别记录ROI面积及相关参数，取3次测量结果平均值作为最终ADC值。

1.4 TIC绘制

在GE Signa HDxt1.5T扫描仪利用乳腺SER软件，在动态增强原始图上选择病灶强化最快、最明显区域作为ROI绘制TIC，ROI大小根据病灶大小调整。参照Thomassin-Naggara[5]分型将TIC分3种类型：I型，缓慢上升，无峰值出现；II型，平台上升；III型：迅速上升，并迅速下降。

1.5 3D减影增强T_1WI

将所有图像传至GEADW4.6后处理工作站，由2名主治医师对动态增强动脉期原始图与增强前平扫原始图像进行相减得到图像。

1.6 统计学分析

采用SPSS19.0软件对研究中得到的数据进行统计学分析，两组计量结果比较采用t检验，计数资料比较采用χ^2检验，P<0.05为差异具有统计学意义。

2 结 果

2.1 肿瘤病理诊断

51例患者55个囊腺类病灶中，囊腺瘤39例，其中浆液性囊腺瘤29例，粘液性囊腺瘤9例，浆液-粘液性囊腺瘤1例，影像学诊断正确率为89.74%(35/39)，2例误诊为囊腺癌，2例误诊为巧克力囊肿。囊腺癌12例，其中交界性1例，高级别11例，影像学诊断正确率为83.33%(10/12)，2例误诊为囊腺瘤。

2.2 常规MRI表现

本组39例囊腺瘤多为圆形或椭圆形，囊壁完整，直径3~23 cm，15例>10 cm，其中单房19例，双房3例，3房以上17例，肿块呈长T_1长T_2信号，分隔呈等T_1短T_2信号，其中19例含分隔，分隔纤细，直径2~3 mm（其中2例>3 mm），9例见彩色玻璃征（图1），6例在T_2WI可见低信号壁结节共15个，直径0.4~1.0 cm，边缘光整（图2），2例囊壁羊齿状突起，3例出现高-略低液平面（图3）。囊腺癌为多房囊实性肿块，形态椭圆形或不规则形，囊壁不均匀增厚，直径0.3~1.3 cm，分隔不均匀增厚，直径4~8 mm，多发壁结节及并局部形成实性肿块，直径1.5~4.6 cm。肿块呈混杂信号，囊性部分呈稍长T_1稍长T_2信号，实性部分呈等或稍短T_1短T_2信号（图4）。

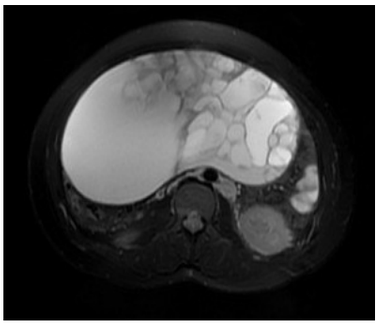

图1 患者，女，23岁，手术证实为右侧黏液性囊腺瘤
Fig.1 Image from 23-year-old female patient with the right mucious cystadenoma confirmed by surgery

T_2-weighted image (T_2WI) showed multilocular appearance, differences of water and mucus signals, forming "stained glass" sign.

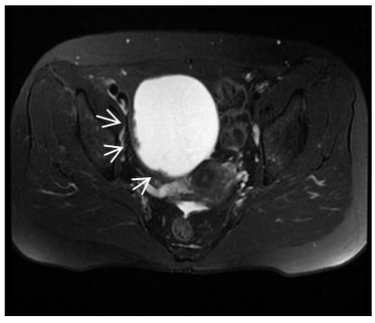

图2 患者，女，47岁，手术证实为右侧浆液性囊腺瘤
Fig.2 Image from 47-year-old female patient with the right serous cystadenoma confirmed by surgery

Fat-suppressed T_2WI revealed multiple low signal nipple nodules (white arrows).

2.3 多b值DWI及ADC特点

随着b值升高，DWI显示囊腺癌囊性部分及囊腺瘤信号不同程度下降（图5和图6），6例囊腺瘤T_2WI显示15个低信号壁结节中仅5个小壁结节信号略升高，余10个壁结节信号无改变，为低信号，囊腺癌不均匀增厚囊壁、壁结节及实性肿块信号明显上升，壁结节及实性肿块内见分支状等低信号；DWI在b值100、500、1 000 mm²/s，卵巢囊腺癌的囊、实性部分ADC低于囊腺瘤瘤体（图7和图8），囊腺瘤ADC分别为$(3.03\pm0.23)\times10^{-3}$、$(2.92\pm0.20)\times10^{-3}$、$(2.88\pm0.21)\times10^{-3}$ mm²/s，囊腺癌囊性ADC分别为$(2.71\pm0.31)\times10^{-3}$、$(2.63\pm0.27)\times10^{-3}$、$(2.47\pm0.41)\times10^{-3}$ mm²/s，囊腺癌实性ADC分别为$(1.80\pm0.50)\times10^{-3}$、$(1.47\pm0.48)\times10^{-3}$、$(1.30\pm0.39)\times10^{-3}$ mm²/s，囊腺瘤的瘤体与囊腺癌的囊、实性ADC值差异均有统计学意义（$P<0.05$）。本组研究中5例囊腺瘤分隔随着b值升高，DWI信号减低、放大。

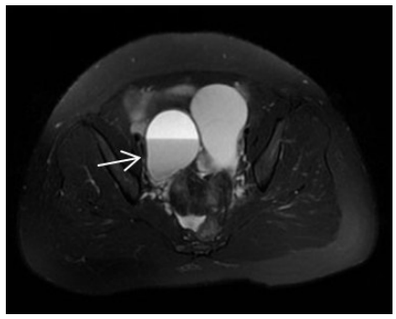

图3 患者，女，47岁，手术证实为双侧浆液性囊腺瘤
Fig.3 Image from 47-year-old female patient with bilateral serous cystadenoma confirmed by surgery

The right ovarian lesions appeared high and low liquid plane on T_2WI, and the low signal on image was considered as mucus deposition.

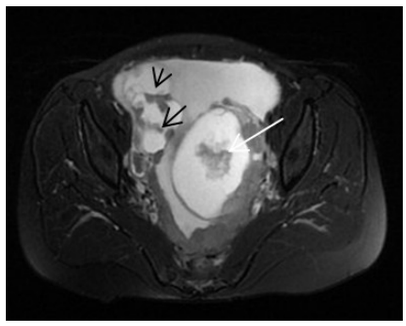

图4 患者，女，44岁，手术证实为双侧高级别浆液性囊腺癌
Fig.4 Image from 44-year-old female patient with bilateral high-grade serous cystadenocarcinoma confirmed by surgery

T_2WI showed low signal wall nodules (black arrows) and cauliflower mass (white arrow).

2.4 DCE、TIC及3D减影增强

DCE显示6例囊腺瘤T_2WI显示15个低信号小

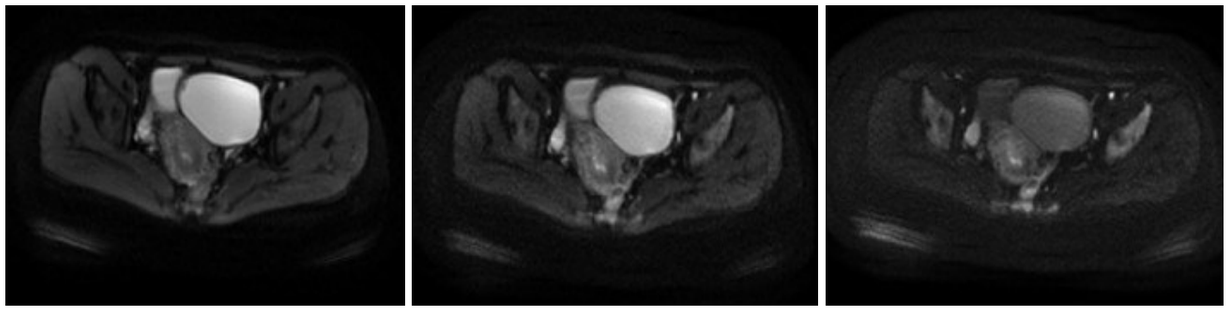

a: b=100 mm²/s b: b=500 mm²/s c: b=1 000 mm²/s

图5 患者，女，30岁，手术证实左侧黏液性囊腺瘤

Fig.5 Image from 30−year−old female patient with left mucious cystadenoma confirmed by surgery

The diffusion-weighted imaging (DWI) signals were gradually decreased.

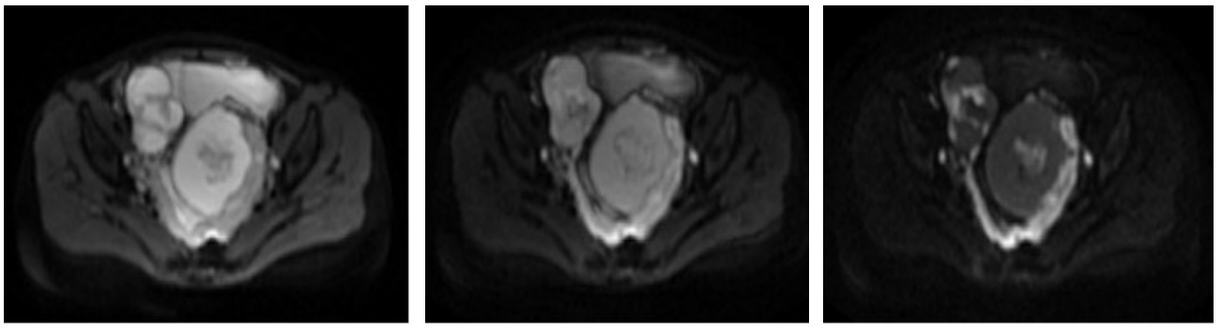

a: b=100 mm²/s b: b=500 mm²/s c: b=1 000 mm²/s

图6 与图4同一患者，分别为b=100、500、1 000 mm²/s时，壁结节、实性部分及肿瘤周围腹膜DWI信号逐渐升高，囊性部分DWI信号逐渐减低

Fig.6 Image from the same patient as Fig.4. b=100, 500, 1 000 mm²/s, the ADC signals of wall nodule, solid components, and peritoneal DWI signals around the tumors were gradually increased, but the DWI signal of cystic component were gradually decreased

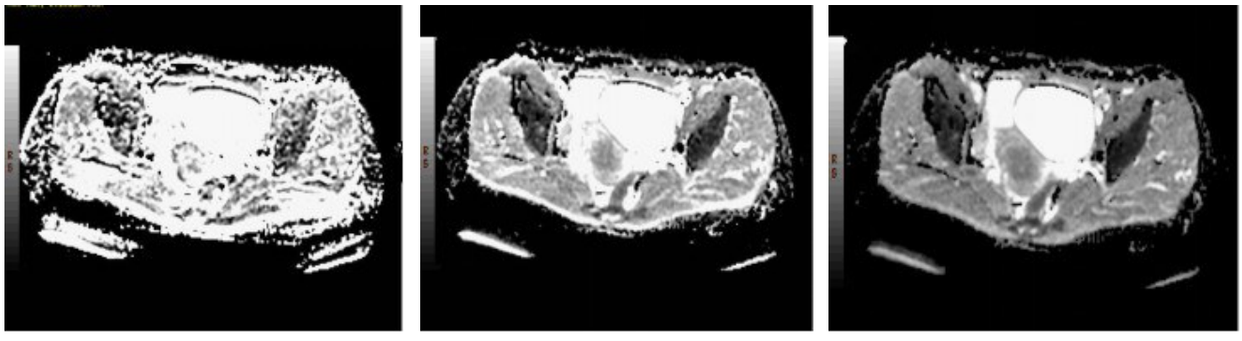

a: b=100 mm²/s b: b=500 mm²/s c: b=1 000 mm²/s

图7 与图5同一患者，对应b=100、500、1 000 mm²/s所得ADC值，显示ADC图信号逐渐升高

Fig.7 Image from the same patient as Fig.5. The ADC value of b=100, 500, 1 000 mm²/s indicates that ADC image signal was gradually increased

壁结节中仅5个小壁结节轻度强化，10个小壁结节无强化，囊壁及分隔渐进性轻-中度强化，TIC类型为I型（图9），11例囊腺癌增厚囊、壁结节及实性肿块动脉期明显强化，并持续强化，1例交界性囊腺癌壁结节动脉期呈轻度强化，并渐进性强化。11例囊腺癌增厚囊壁、壁结节及实性肿块TIC类型为II型曲线（图10），1例交界性囊腺瘤TIC类型为I型。3D减影清楚显示壁结节动脉期强化特点，囊腺瘤乳头结构轻度强化，血栓及细胞碎片无强化，囊腺癌壁结节及肿块明显强化。本组6例乳头结构动脉期轻度强化，1例交界性囊腺癌动脉期轻度强化，11例囊腺癌壁结节及实性部分动脉期明显强化。

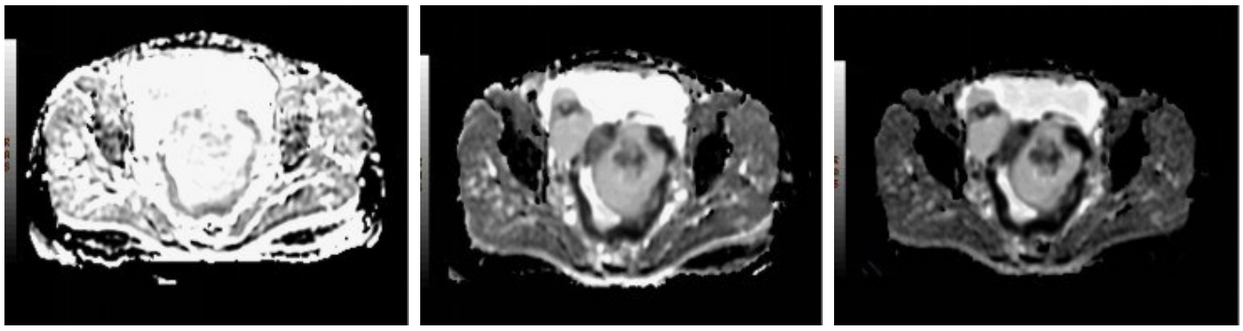

d: b=100 mm²/s　　e: b=500 mm²/s　　f: b=1 000 mm²/s

图8 与图4同一患者，对应b=100、500、1 000 mm²/s所得ADC值，壁结节、实性部分及肿块周围腹膜ADC图信号逐渐减低，囊性部分表现为高信号

Fig.8 Image from the same patient as Fig.5. b=100, 500, 1 000 mm²/s, the ADC of wall nodule, solid components, and peritoneal ADC around the mass was gradually decreased, but the cystic component appeared high signals

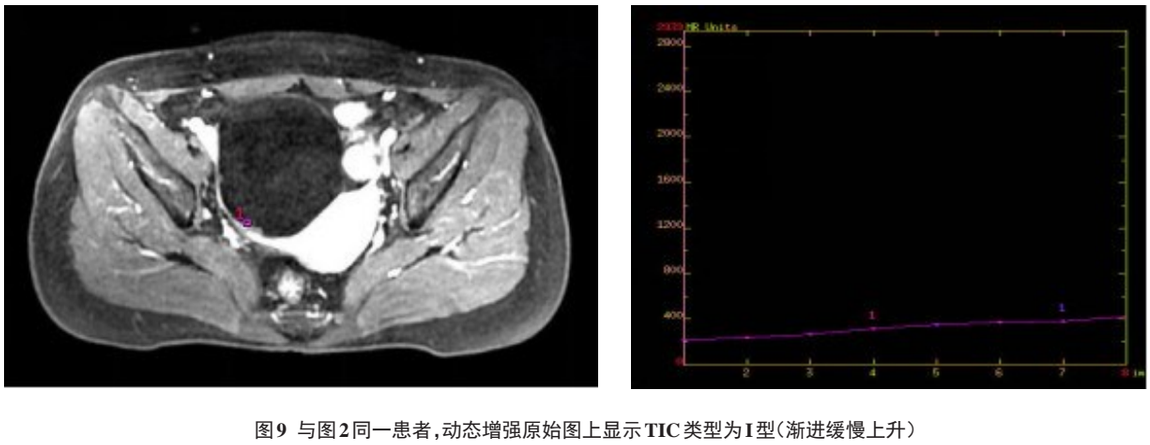

图9 与图2同一患者，动态增强原始图上显示TIC类型为I型（渐进缓慢上升）

Fig.9 Image from the same patient as Fig.2. The dynamic contrast-enhanced original image shows that the TIC is type I (progressive and slow rise)

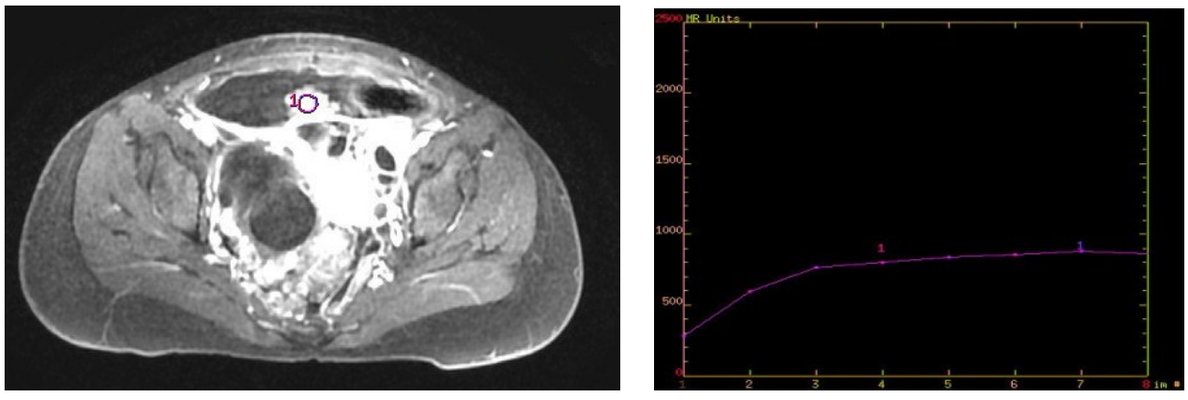

图10 患者，女，32岁，手术证实右侧高级别浆液性囊腺癌

Fig.10 Image from 32-year-old female patient with right high-grade serous cystadenocarcinoma confirmed by surgery

The dynamic contrast-enhanced original image showed that the TIC was type II (platform rise).

3 讨 论

3.1 常规MRI表现

囊腺瘤中浆液性表现为单房或多房。本组29例浆液性囊腺瘤中12例多房，囊壁薄，呈长T_1、长T_2水样信号，本组3例病灶后下部见斑片状短T_1信号，T_2WI信号相应减低呈等或低信号，形成高-稍低液平面，结合病理，其中1例因为肿瘤蒂扭转肿瘤内出血形成，另外2例结合项剑瑜等[6]报道，笔者认为与黏

液蛋白沉积有关。黏液性囊腺瘤一般为多房。本组10例黏液性囊腺瘤(包括1例浆液-黏液性囊腺瘤)中2例为单房,8例为多房。Outwater等[7]在影像研究中发现黏液性囊性肿瘤显示特征多房外观,水液性成分呈长T_1、长T_2信号,黏稠的黏蛋白成分呈短T_1、稍长或稍短T_2信号,呈现"彩色玻璃外观",本组有5例黏液性囊腺瘤和4例多房浆液性囊腺瘤中均发现此征象。囊腺瘤囊壁偶尔可形成乳头突起,T_2WI呈低信号。随着b值升高,DWI显示瘤体信号不同程度减低。囊腺癌表现为囊实性肿块,囊壁不均匀增厚、形成壁结节及肿块,T_1WI呈等信号,T_2WI呈低信号,边缘分叶。随着b值升高,DWI显示囊性部分信号不同程度减低,增厚囊壁、壁结节、肿块信号不同程度升高。

3.2 多b值DWI、ADC值意义

定量DWI和ADC值鉴别良恶性病变有无意义存在一定争议。Bakir[8]和Kim[9]研究发现,由于(1)肿瘤内含有血液及含铁血黄色等顺磁性物质,(2)卵巢囊腺类肿瘤囊液内黏液、浆液、蛋白浓度,(3)肿瘤的坏死及囊变、纤维细胞、胶原纤维,这3种原因均会影响ADC值,因此ADC平均值在卵巢恶性肿瘤与卵巢良性肿瘤存在重叠性,但张奕伟[10]、Li[11]、Zhang[12]等认为卵巢恶性囊腺类肿瘤实性ADC值低于卵巢良性囊腺类肿瘤有一定意义。Koh等[13]认为由于DWI的参数会直接影响ADC值,b值选择很重要。本组研究设定3个b值,分别为100、500、1 000 mm^2/s,测量51例55个病灶,研究结果显示卵巢囊腺癌囊、实性部分ADC均低于囊腺瘤,且有显著统计学意义(P<0.05),研究结果与文献[10-12]报道相似。笔者认为多b值表现ADC值比单b值所表现ADC值对诊断囊腺瘤和囊腺癌有较大的意义。本组5例囊腺瘤分隔随着b值升高,DWI信号减低、放大,考虑与铁血黄素沉着有关。

3.3 DCE及TIC类型的价值

Franiel等[14]认为DCE能定性、半定量、定量评估卵巢肿瘤血流灌注不同增强模式,形成不同类型TIC曲线,从而鉴别卵巢良恶性肿瘤,He[3]和Hansford[4]等将DCE的TIC类型广泛用于鉴别乳腺和前列腺良恶性肿瘤,并取得一定临床价值。此技术少在卵巢肿瘤中运用。Malek等[15]研究发现TIC类型是一种比较准确诊断卵巢良恶性的技术。Malek[15]及Li[16]等发现卵巢恶性肿瘤动态增强后TIC曲线为III型,良性为I型,交界性I或II型。本组13个囊腺癌动态增强后壁结节及实性肿块呈快速明显强化,曲线呈II型,2个交界性囊腺瘤壁结节呈渐进性强化,表现为I型,6例囊腺瘤中5个小壁结节动态增强轻度强化,曲线呈I型。但由于病例过少,得出的曲线虽与文献相仿,但还需大量样本数据支持。本组研究13个囊腺癌TIC曲线II形态与文献[15-16]结果相违背,但与郭永梅等[17]研究结果相符合。笔者认为TIC类型I型对卵巢良性肿瘤有明确诊断价值,而恶性肿瘤表现为II和III型,因此TIC类型曲线是评估卵巢良恶性肿瘤的一种可靠的检查方式,比DWI和ADC值更精确,但是良性病变与交界性病变存在重叠性,所以结合多b值DWI和ADC可进一步提高评估卵巢良恶性肿瘤准确性。

3.4 3D减影增强意义

卵巢囊腺瘤偶尔可见乳头壁结节,主要为纤维核,T_2WI表现为低信号。当其生长突起明显,应考虑为交界性囊腺癌,交界性囊腺癌临床表现为良性。Geze等[18]报道3D减影技术有助于发现细胞碎片或血栓及突变乳头壁结节。由于细胞碎片及血栓无强化,纤维核动脉期轻度强化,恶性壁结节动脉期明显强化[19],本组6例14个T_2WI为低信号乳头壁结节,2例囊壁羊齿状突起,仅有5个乳头壁结节轻度强化,考虑为纤维核,10个乳头壁结节及2例囊壁羊齿状突起无强化,考虑为血栓或细胞碎片,与Geza[18]的报道一致。

综上所述,MRI动态增强扫描、多b值DWI结合ADC值、TIC曲线类型、3D减影技术联合应用,对鉴别卵巢囊腺瘤和囊腺癌有重要的作用及价值,较大程度提高了卵巢良恶性诊断准确率,可作为妇科肿瘤重要的检查方法。

【参考文献】

[1] 卞读军, 肖恩华. 磁共振扩散成像技术及其在肝癌的临床应用[J]. 国际医学放射学杂志, 2011, 34(5): 439-444.
BIAN D J, XIAO H. Clinical application of diffusion- weighted imaging in hepatocellular carcinoma[J]. International Journal of Medical Radiology, 2011, 34(5): 439-444.

[2] THOMASSIN-NAGGARA I, DARAI E, CUENID C A, et al. Contribution of diffusion-weighted MR imaging for predicting benignity of complex adnexal mass[J]. Eur Radiol, 2009, 19(6): 1544-1552.

[3] HE D F, MA D Q, JIN E H. The use of dynamic contrast enhanced MRI in differentiating between benign and malignant breast tumors and predicting the histologic grade for breast cancer patients[J]. Chin J Radiol, 2012, 46(12): 1075-1078.

[4] HANSFORD B G, PENG Y, JIANG Y, et al. Dynamic contrast-enhanced MR imaging curve-type analysis: is it helpful in the differentiation of prostate cancer from health peripheral zone[J]. Radiology, 2015, 275(2): 448-457.

[5] THOMASSIN-NAGGARA I, DARAI E, CUENID C A, et al. Dynamic contrast- enhanced magnetic resonance imaging: a useful tool for characterizing ovarian epithelial tumors[J]. J Magn Reson Imaging,

2008, 28(1): 111-120.
[6] 项剑瑜, 刘绪明, 余捷, 等. MRI在卵巢良性与交界性黏液性囊腺瘤鉴别诊断中的价值[J]. 中华内分泌外科杂志, 2015, 9(3): 219-222.
XIANG J Y, LIU X M, YU J, et al. Value of MRI in differentiation diagnosis of benign ovarian and borderline mucinous cystadenoma [J]. Journal of Endocrine Surgery, 2015, 9(3): 219-222.
[7] OUTWATER E K, SCHIEBLER M L. Magnetic resonance imaging of the ovary[J]. Top Magn Reson Imaging, 2001, 12(2): 131-146.
[8] BAKIR B, BAKAN S, TUNACI M, et al. Diffusion-weighted imaging of solid or predominantly solid gynaecological adnexial masses: is it useful in the differential diagnosis[J]. Br J Radiol, 2011, 84(1003): 600-611.
[9] KIM H J, LEE S Y, YU R S, et al. The value of diffusion-weighted imaging in the differential diagnosis of ovarian lesions: a Meta-analysis [J]. PLoS One, 2016, 11(2): 10-23.
[10] 张奕伟, 郑少燕, 吴先衡, 等. 常规MRI结合DWI鉴别诊断卵巢良恶性囊腺类肿瘤[J]. 中国医学影像技术, 2013, 29(10): 1691-1694.
ZHANG Y W, ZHENG S Y, WU X H, et al. Routine MRI combining DWI for differential diagnosis of benign and malignant ovarian cystadenomatous tumors[J]. Chinese Journal of Medical Imaging Technology, 2013, 29(10): 1691-1694.
[11] LI W, CHU C, CUI Y, et al. Diffusion-weighted MRI: a useful technique to discriminate benign *versus* malignant ovarian surface epithelial tumors with solid and cystic components[J]. Abdom Imaging, 2012, 37(5): 897-903.
[12] ZHANG P, CUI Y, LI W, et al. Diagnostic accuracy of diffusion-weighted imaging with conventional MR imaging for differentiating complex solid and cystic ovarian tumors at 1.5 T[J]. World J Surg Oncol, 2012, 10(1): 237-245.
[13] KOH D M, COLLINS D J. Diffusion-weighted MRI in the body: applications and challenges in oncology[J]. AJR Am J Roentgenol, 2007, 188(6): 1622-1635.
[14] FRANIEL T, HAMM B, HRICAK H. Dynamic contrast-enhanced magnetic resonance imaging and pharmacokinetic models in prostate cancer[J]. Eur Radiol, 2011, 21(3): 616-626.
[15] MALEK M, POURASHRAF M, MOUSAVI A S, et al. Differentiation of benign from malignant adnexal masses by functional 3 tesla MRI techniques: diffusion-weighted imaging and time-intensity curves of dynamic contrast-enhanced MRI[J]. Asian Pac J Cancer Prev, 2015, 16(8): 3407-3412.
[16] LI H M, QIANG J W, MA F H, et al. The value of dynamic contrast-enhanced MRI in characterizing complex ovarian tumors[J]. J Ovarian Res, 2017, 10(1): 4-11.
[17] 郭永梅, 黄云海, 魏新华, 等. 3.0T动态增强磁共振对卵巢肿瘤的半定量及定量分析研究[J]. 磁共振成像, 2015, 6(10): 782-786.
GUO Y M, HUANG Y H, WEI X H, et al. Semi-quantitative and quantitative parametric analysis of 3.0T dynamic contrast-enhanced magnetic resonance imaging in diagnosing tumors of ovary [J]. Chinese Journal of Magnetic Resonance Imaging, 2015, 6(10): 782-786.
[18] GEZE A. Serous and mucinous borderline (low malignant potential) tumors of the ovary[J]. Am J Clin Pathol, 2005, 123: 13-57.
[19] THOMASSIN-NAGGARA I, BALVAY D, AUBERT E, et al. Quantitative dynamic contrast-enhanced MR imaging analysis of complex adnexal masses: a preliminary study[J]. Eur Radiol, 2012, 22(4): 738-745.

（编辑：黄开颜）